Available online at www.sciencedirect.com
ScienceDirect
Journal of the European Ceramic Society 27 (2007) 2463–2469
www.elsevier.com/locate/jeurceramsoc

Anisotropy on $SrTiO_3$ templated textured PMN–PT monolithic ceramics

E.R.M. Andreeta [a,*], H.F.L. dos Santos [a], M.R.B. Andreeta [b], M.H. Lente [a], D. Garcia [a], A.C. Hernandes [b], J.A. Eiras [a]

[a] *Grupo de Cerâmicas Ferroelétricas, DF/UFSCar, Rod. Washington Luis, 235, São Carlos-SP 13565-905, Brazil*
[b] *Grupo de Crescimento de Cristais e Materiais Cerâmicos, IFSC/USP P.O. Box 369, São Carlos-SP 13560-970, Brazil*

Received 21 May 2006; received in revised form 20 September 2006; accepted 7 October 2006
Available online 1 December 2006

Abstract

In this work, templated grain growth (TGG) and reactive templated grain growth (RTGG) texture techniques combined with uniaxial hot pressing were used for the first time to produce high dense monolithic textured 0.6PMN–0.4PT ceramics. Microstructural analysis of the textured ceramics showed that both TGG and RTGG texture methods are efficient to promote anisotropic grain nucleation around the $SrTiO_3$ single crystal templates. The structural data remarkably revealed that although there was no previous reaction of the powder to form the lead magnesium niobate–lead titanate (PMN–PT) compound in the RTGG samples and the ceramic phase formation was 100% perovskite indicating that RTGG texture technique is more attractive than TGG in the case of $SrTiO_3$ templated PMN–PT. Rather, dielectric characterizations performed in the RTGG samples parallel and perpendicular to the template axis revealed a high anisotropy in the electrical permittivity for RTGG samples (1.48) that were comparable to an estimated value for 0.62PMN–0.38PT single crystals. Piezoelectric characterization of RTGG samples resulted in strain levels up to 0.34% and the highest d_{33} coefficient was 1100 pC/N, which showed significant increase compared to random ceramic.

Keywords: Grain growth; Hot pressing; Dielectric properties; Perovskites; Texture

1. Introduction

Over the last decades, the development of functional ceramic materials has opened a wide range of new possible technological applications. In this context, lead based ferroelectric materials are massively being used in several electronic devices such as pyroelectric sensors, piezoelectric actuators and electro-optical components.[1,2]

The anisotropic properties of these ferroelectric materials in single crystal form provide excellent opportunities for improvements in electro electronic industry, but the costs of production are higher than the ones for ceramics. On the other hand, due to the random crystallographic orientation of bulk ceramics they present an average of the directionally dependent physical properties, and engineering of ferroelectric domains cannot be achieved unless texture can be introduced. Ceramics textured by templated grain growth (TGG) may present anisotropic properties similar to those of single crystals.[3–5] The TGG technique consists in the orientation of single crystal templates in a finer-size particles matrix[6] and it is an interesting way to reduce the cost of single crystal-like materials.

Among the ferroelectric materials of texture interest, the complex perovskite lead magnesium niobate [$Pb(Mg_{1/3}Nb_{2/3})O_3$ or PMN] has emerged as a high quality material due to its excellent electrical and electromechanical properties.[7] However, PMN ceramics are difficult to obtain in a pure ferroelectric phase due to the formation of a stable paraelectric phase (pyroclore) during the sintering process. Nevertheless, the columbite powder preparation method developed by Swartz and Shrout[8] combined with the addition of $PbTiO_3$ (PT) to form $(1-x)PbMg_{1/3}Nb_{2/3}O_3$–$(x)PbTiO_3$ solid solution (lead magnesium niobate–lead titanate, PMN–PT) have been revealed a useful route to stabilize the perovskite phase. Thus, the PMN–PT can present high dielectric and piezoelectric constants, especially around the morphotropic phase boundary.[9,10] Ferroelectric single crystals of PMN–PT present very high piezoelectric coefficients for specific cutting and poling conditions,[3] but predictions on the effective piezoelectric

* Corresponding author. Tel.: +55 16 3351 8227; fax: +55 16 3368 4997.
E-mail address: erika@df.ufscar.br (E.R.M. Andreeta).

0955-2219/$ – see front matter © 2006 Elsevier Ltd. All rights reserved.
doi:10.1016/j.jeurceramsoc.2006.10.011

coefficients and electromechanical coupling factors of PMN–PT ceramics with [0 0 1], [0 1 1] and [1 1 1] fiber textures have been made and the results are comparable to the ones obtained for single crystals.[11]

Tape casting combined with TGG and reactive TGG (RTGG) processes has recently succeeded to prepare high crystallographic oriented PMN–PT ceramics.[3,12,13] Sabolsky et al.[3] have used templates of $BaTiO_3$ with success in the production of PMN–PT textured ceramics by RTGG, which is a variation of TGG, where the matrix is a precursor of the final phase. The $SrTiO_3$ templated PMN–PT achieved high texture degree but the reactivity of the template with the matrix decreased the maximum dielectric constant and transition temperature.[6,12] Besides, tape casting processes result in thick ceramics, which makes very difficult the measurements of anisotropy caused by texture.

In this work, the combination of TGG and RTGG techniques with uniaxial hot pressing for the sinterization process was tested to texture lead magnesium niobate–lead titanate monolithic ceramics without reaction between templates and matrix. The templates used for the texture process of the PMN–PT ceramics were obtained from $SrTiO_3$ single crystals fibers, grown by the laser heated pedestal growth technique (LHPG).[14] The texturing of the obtained samples was investigated by microstructural, dielectric and piezoelectric characterizations. Anisotropy on dielectric and piezoelectric properties are shown in PMN–PT textured ceramics.

2. Experimental procedure

The experimental procedure was divided in the single crystal fibers growth to obtain the templates, the obtaining of the $SrTiO_3$ templated PMN–PT samples and their characterization. Fig. 1 shows a schematic draw of the main steps of the production of the textured ceramics.

The $SrTiO_3$ templates were obtained from single crystal fibers grown by the laser heated pedestal growth technique. The pedestals (source material) used in the $SrTiO_3$ single crystal fibers growth process were produced by the mixture of stoichiometric amounts of $SrCO_2$ (Merk Optipur) and TiO_2 (Vetec 99.8%) before a cold extrusion process. These pedestals were used in the growth process without any prior synthetization or sintering process. These two steps, plus the crystal pulling itself, can be reduced in just one step in the LHPG technique.[15] The $SrTiO_3$ fibers grown were 500 μm in diameter and around 6 cm in length. The preferential growth orientation of these fibers is [1 1 0].[16] The fibers were then cut in 3:1 aspect ratio pieces in order to produce the templates.

PMN–PT powder used for the densification through TGG technique was prepared by the columbite method, which consists of the previous reaction of the Nb_2O_5 (CBMM 99.4%) and the $Mg(NO_3)_2{\cdot}6H_2O$ (Merck 99%) in order to produce the $MgNb_2O_6$. The magnesium niobium oxide was then mixed and reacted with the PbO (Aldrich >99.9%) and the TiO_2 (Aldrich >99.9%) to form the 0.6PMN–0.4PT. This composition was chosen because it is near to the PMN–PT morphotropic phase boundary region. The powder was milled with zircon balls until it achieves submicrometric dimensions. The powder used in the RTGG experiments was prepared using the simple mix of the lead, titanium and magnesium niobium oxides without previous reaction. For the RTGG samples in which heat treatment was performed, to the non-reacted powder 3 wt% excess of PbO was added in order to increase the liquid phase during the treatment and to improve the grain growth kinetics.[6] Both types of powder were then uniaxially and isostatically pressed at room temperature with 3 vol% $SrTiO_3$ single crystal

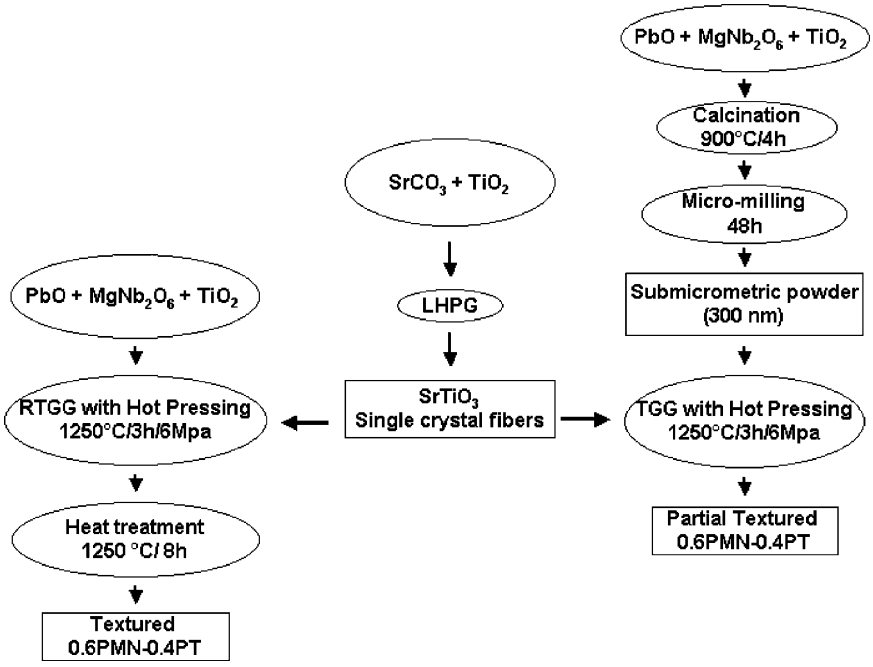

Fig. 1. Scheme of the experimental procedure used to obtain texturing on PMN–PT ceramics.

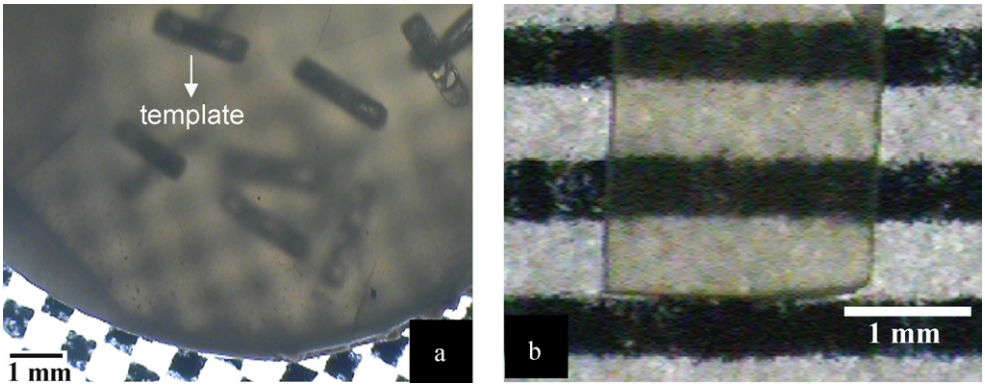

Fig. 2. PMN–PT samples obtained through TGG and hot press combined methods. (a) 0.625PMN–0.375PT translucent ceramic body after densification, with the templates aligned perpendicularly to the press axis. (b) Cut 0.6PMN–0.4PT translucent sample.

templates inside to produce the green ceramic bodies. After the powder conformation, all the templates were aligned with their pulling axis perpendicular to the press axis. The other axes (perpendicular to pulling axis) were not physically aligned among the templates. It means that the templates were randomly oriented inside the green ceramic body, as it can be seen in Fig. 2a.

The densifications of the ceramics were performed in a Uniaxial Hot Press Thermal Inc. system, under conditions of 1250 °C/3 h/6 MPa under a controlled oxygen atmosphere. Post-sintering heat treatments on RTGG samples were performed under 1250 °C/8 h conditions. The microstructures of the samples were observed through a JEOL scanning electronic microscopic (SEM). The temperature dependence of the electrical permittivity of the textured samples was characterized at 1 kHz employing an Impedance Analyzer HP 4194A and a homemade furnace at a controlled cooling of 2 °C/min. The electric field-induced strain measurements were performed employing a MIT-2000 Fotonic Sensor, applying a triangular electric field of amplitude of 20–30 kV/cm at 100 mHz and at room temperature. The dielectric and piezoelectric measurements were made in different samples directions in order to evaluate the degree of anisotropy of the textured ceramics. For 0.6PMN–0.4PT samples produced by RTGG and hot pressing, X-ray diffractometry measurements were performed using a Siemens D500 diffractometer in order to confirm the perovskite (ferroelectric phase) PMN–PT formation.

3. Results and discussion

The X-ray diffractometry results performed on RTGG samples showed that the ceramics presented only the perovskite structure without any pyroclore phase, as seen in Fig. 3. The peaks were indexed using the International Centre of Diffraction Data (JPCPDF-ICDD). The PMN–PT monolithic ceramic samples obtained by TGG and hot pressing technique were highly dense and translucent, as shown in Fig. 2. The translucence observed on the ceramics is evidence of clean grain boundaries, a homogenous microstructure and low porosity.

The SEM micrographs of 0.6PMN–0.4PT transversal section (perpendicular to press axis) ceramic samples, produced by both TGG or RTGG texture processes combined with hot pressing, can be seen in Fig. 4. A comparison between the average grain size for ceramics prepared by TGG and RTGG showed that the grains of the RTGG sample are smaller than the ones of TGG ceramics sintered during same time, as it is illustrated in Fig. 4b and d. This happens due to the smaller grain growth time in the RTGG technique when compared to the TGG process. In the sintering process by TGG, the powder is pre-reacted and the phase PMN–PT phase is already established. On the other hand, in the RTGG the chemical reaction and the formation of the PMN–PT phase must occur before the grain growth process. Considering that the time available for annealing in both processes were the same, the effective time for the grain growth in the RTGG technique was, in fact, smaller.

The micrographs of Fig. 4a and c show the preferred grain nucleation on the vicinities of the template/ceramic boundary, indicating the effectiveness of the $SrTiO_3$ single crystal fiber templates as seed for the PMN–PT grains orientation. In both samples, the grain size near the templates is much larger when compared with grains in a position far from any template, Fig. 4b and d. The average grain size was measured for TGG and RTGG samples in positions far and near templates, using different micrographs. For TGG sample the average grain size was 9.0 and

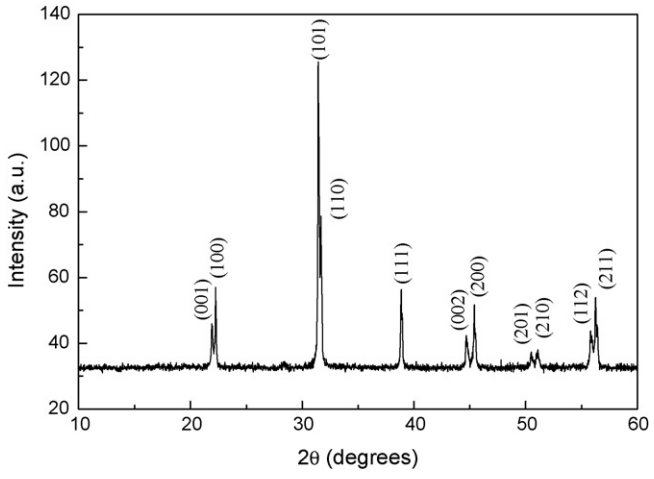

Fig. 3. X-ray diffractometry of a 0.6PMN–0.4PT sample with $SrTiO_3$ templates, made by RTGG plus uniaxial hot pressing techniques.

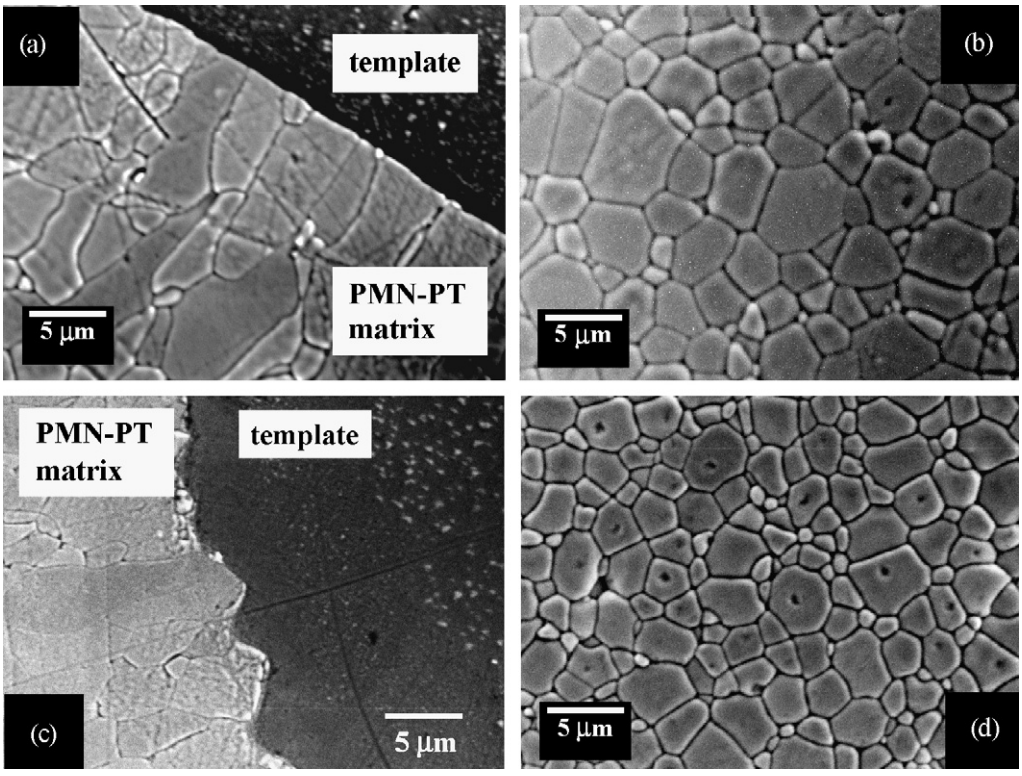

Fig. 4. Micrographs of 0.6PMN–0.4PT samples produced by TGG and RTGG techniques combined with uniaxial hot pressing. (a) Grain near a template in TGG sample. (b) Grains of TGG sample in region far from templates. (c) Grain near a template in RTGG sample. (d) Grains in region far from templates of RTGG sample.

3.1 μm near and far from templates, respectively, and for RTGG sample those values were 8.3 and 1.9 μm. The ratios between grain sizes near and far from templates are 2.9 for TGG and 4.4 for RTGG samples. Those results indicate that the RTGG technique appears to be more efficient than TGG in order to use the $SrTiO_3$ as a seed and to promote the PMN–PT grain growth, when comparing the grain size around a template to the grains far from templates. The process that occurs during templated grain growth is the exaggerated grain growth in a liquid phase, where large grains or particles grow at the expense of finer grains. The driving force for TGG processes is given by the difference in surface free energies between the matrix grains and the advancing crystal plane.[6,13] Seabaugh and co-workers presented a model which shows that this driving force decreases during TGG processes while matrix coarsening.[6] This model also shows that there is a strong influence of the matrix grain size during TGG. It means that the finer the matrix grain size, the higher the driving force for TGG. In this way, the smaller average grain size of the PMN–PT ceramics produced by hot pressing and reactive TGG propitiated a higher driving force than TGG samples. Plus, since the matrix seeded has the same crystallographic orientation that the template, the effective volume of oriented grains prior to densification can be greater in RTGG than with TGG.[6] Due to better grain size gain obtained in the RTGG ceramics and its easier powder preparation process, only the samples prepared by this technique were used to continue the present study.

RTGG and hot pressing could improve PMN–PT grain growth with heat treatment after the sample sintering. The conditions of this treatment were 1250 °C under oxygen atmosphere for 8 h. Fig. 5 shows a comparison of the PMN–PT grain growth from templates before and after heat treatment, where it can be seen that the average grain size near the templates increased from 9 to 16 μm in the largest grain axis. The grain growth rate on this axis was 3 μm/h during the sintering under pressure and 0.9 μm/h during the heat treatment. Similar growth rates of Kwon et al. for $SrTiO_3$ templated 0.675PMN–0.325PT were 15 μm/h at the beginning and 0.6 μm/h in the final part of their 50 h process. The difference between the initial growth rates for Kwon et al. and the present work is probably due to the fact that the initial stage of this work process is hot pressed and the grain growth process suffers inhibition from pressure axis direction and also from the dye walls. Plus, the heating rate used by Kwon is 15 °C/min, three times higher than that used in this work. It is known that the firing rate affects the density and grain growth of a ceramic.[17] The higher is the heating rate, higher is the densification rate and smaller is the grain size during sintering. Then, the high rate used by Kwon may cause the appearance of finer grains, which would cause a higher driving force for the TGG process. Our sintering processes in the hot pressing set up has a high thermal inertia, which prevents the use of high heating rates to achieve the conventional sintering temperatures.

Dielectric characterizations allowed the comparison of the dielectric coefficients between three perpendicular directions in ceramics obtained by RTGG and hot pressing. The measurements were performed in unpoled samples cut in regions near to the templates. The two directions measured were both perpendicular to the template axis ([1 1 0] direction) and one of

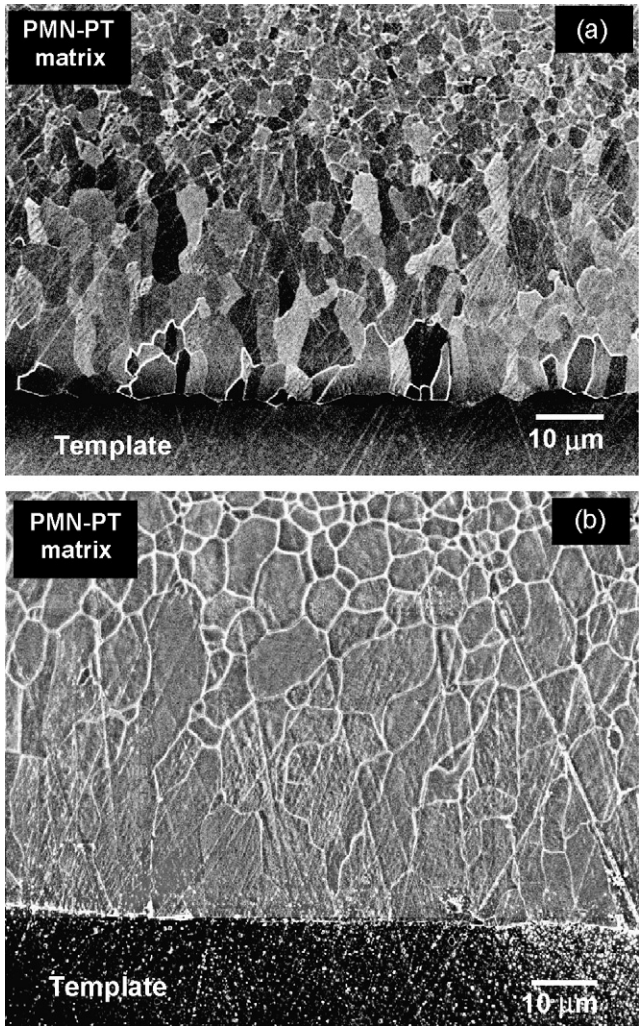

Fig. 5. Grain near a template in 0.6PMN–0.4PT samples produced by RTGG combined with uniaxial hot pressing. (a) Sample with no post-sinterization heat treatment. (b) Sample with 8 h of post-sinterization heat treatment at 1250 °C.

them was parallel to the press axis, as it can be seen in Fig. 6. These results show only a partial anisotropy, which reflected in a higher dielectric constant only near the temperature of the maximum of the dielectric permittivity (peak) for the sample, measured parallel to the pressing axis. One of the disadvantages in working with fiber-like templates during the texturing process is the knowledge of the template orientation only in its pulling axis. Thus, the direction choice to the dielectric measurements must be careful in order to measure anisotropy. The two directions measured (perpendicular to [1 1 0]) could present similar dielectric constants and the anisotropy could then be unnoticed.

The dielectric data in Fig. 7 suggest that the unpoled sample with a post-sintering heat treatment at 1250 °C/8 h presents high anisotropy. Three perpendicular directions were chosen to measure: parallel (parallel to the template axis), perpendicular 1 (perpendicular to the template axis and parallel to the press axis) and perpendicular 2 (perpendicular to both previous directions). Rather, the dielectric constant at room temperature in the perpendicular 1 direction ($\varepsilon_{\perp 1}$) is significantly higher than that for other both directions and the anisotropy factor at room temperature is about 1.5. Moreover, unlike the results from Kwon et al.,[12] neither the maximum of the dielectric constant nor the transition temperature (T_C) are lower than those found for random ceramics.[18] On the contrary, the values of dielectric constant are significantly higher for the textured sample. In Table 1, it can be noticed that the dielectric constant values obtained to the textured 0.6PMN–0.4PT ceramics at room temperature and at transition temperature (T_C) are higher than those found for random ceramics, attesting the high good dielectric quality of the RTGG textured PMN–PT produced in this work. The parallel direction must have a preferential orientation in [1 1 0]. Since the [1 $\bar{1}$ 0] direction does not have any difference in symmetry to [1 1 0] and it is perpendicular to this direction, it can be concluded that the perpendicular 2 direction in Fig. 7 is preferentially [1 $\bar{1}$ 0], due to the similarity of the dependences of the dielectric constant on the temperature. The perpendicular 1 direction (parallel to the press axis) then should be preferentially [0 0 1]. The anisotropy factor obtained in the 0.6PMN–0.4PT ceramic at room temperature is $\varepsilon_{\perp 1}/\varepsilon_{//} = 1.48$.

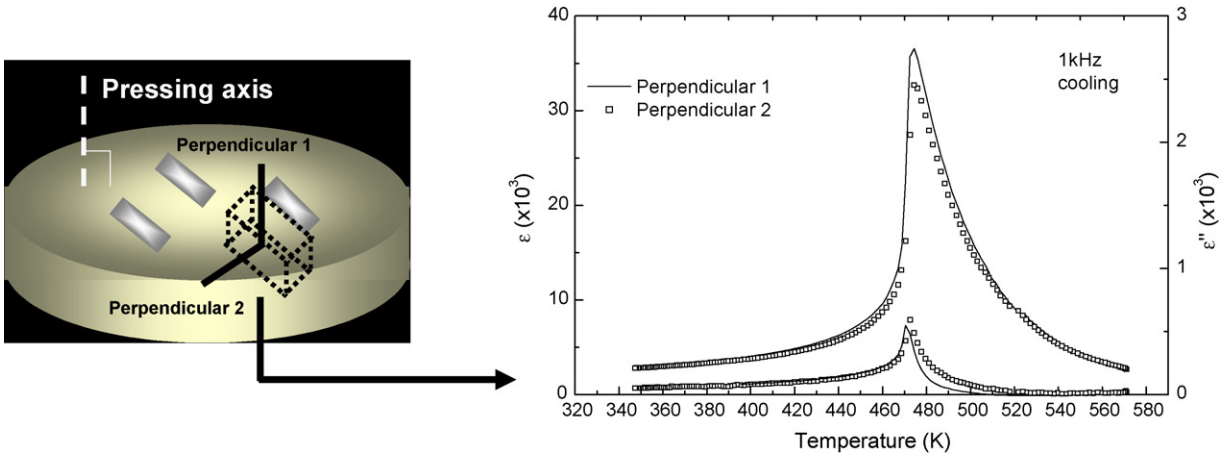

Fig. 6. Dependence of the relative dielectric constant ε' on the temperature for a sample of 0.6PMN–0.4PT prepared by RTGG and hot pressing combined techniques in axes perpendicular to the template axis.

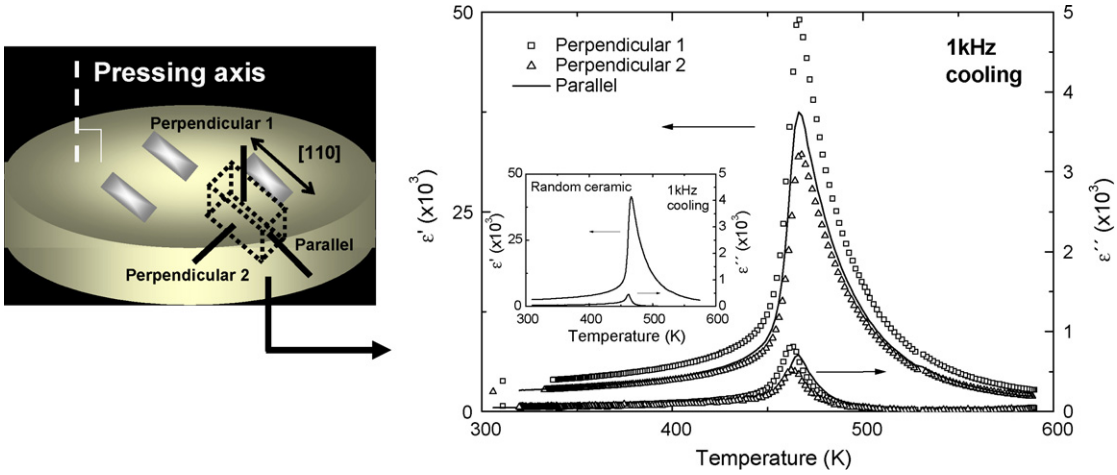

Fig. 7. Dependence of the dielectric constant ε' on the temperature in axis parallel and perpendicular to the template for a sample of 0.6PMN–0.4PT prepared by RTGG plus hot pressing and 8 h of post-sinterization heat treatment. Inserted graphic: dielectric measurement for a random ceramic.

Table 1
Dielectric and piezoelectric properties of random or textured 0.6PMN–0.4PT ceramics and [0 0 1] or [1 1 0]-oriented single crystals[20,21,23]

Sample	Maximum dielectric constant (ε'_{max})	Room temperature dielectric constant	d_{33} (pC/N)
[0 0 1]-0.62PMN–0.38PT single crystal[20,23]	5.0×10^4	6.0×10^3	300
[1 1 0]-0.62PMN–0.38PT single crystal[21,23]	3.4×10^4	4.0×10^3	1200
ST-0.6PMN–0.4PT perpendicular 1	5.0×10^4	4.0×10^3	750
ST-0.6PMN–0.4PT perpendicular 2	3.8×10^4	2.7×10^3	1100
Random 0.6PMN–0.4PT	4.1×10^4	2.5×10^3	840

Up to the authors' knowledge, there is no report of dielectric properties of a 0.6PMN–0.4PT single crystal. Two reports present dielectric characterization of 0.62PMN–0.38PT single crystals, a very similar composition and same structure, for [0 0 1][19] and [1 1 0][20] directions. Although the crystals reported in these two papers have been grown in the same laboratory, there is no guarantee that the dielectric measurements were performed at the same samples. This way, an anisotropy factor can be only estimated to a 0.62PMN–0.38PT single crystal with a value of $\varepsilon_{[0\,0\,1]}/\varepsilon_{[1\,1\,0]} = 1.5$ at room temperature for unpoled samples. It can be noticed that this anisotropy factor is very similar to the one obtained for the textured ceramic presented in this work.

Two important aspects in the dielectric results shown in Figs. 6 and 7 may be concluded. First, these results are a direct evidence of a minimum contamination of the matrix with Sr, which could reduce the values of the dielectric constant.[6,12] Second, the fact that the electrical permittivity of the RTGG textured PMN–PT sample presents a high degree of anisotropy suggests strongly a texturing process of ferroelectric domains. The microstructural texturing of the samples implies a ferroelectric domain texture, which may be understood as an engineered domain configuration process similar to that observed in single crystals, that naturally induces enhanced physical properties of the textured ceramics in specific directions.[22]

The electric field-induced strain curves for perpendicular 1 and 2 directions of the same sample presented in Fig. 7 are shown in Fig. 8. The anisotropy between perpendicular 2 and 1 directions can be seen, as well the improvement achieved in direction perpendicular 2 comparing to a random ceramic. The textured ceramic showed maximum strain of about 0.34% at 25.5 kV/cm in perpendicular 2 direction and about 0.22% of maximum strain at 29 kV/cm in perpendicular 1 direction. The maximum strain value for the random ceramic was 0.24% at 21.5 kV/cm.

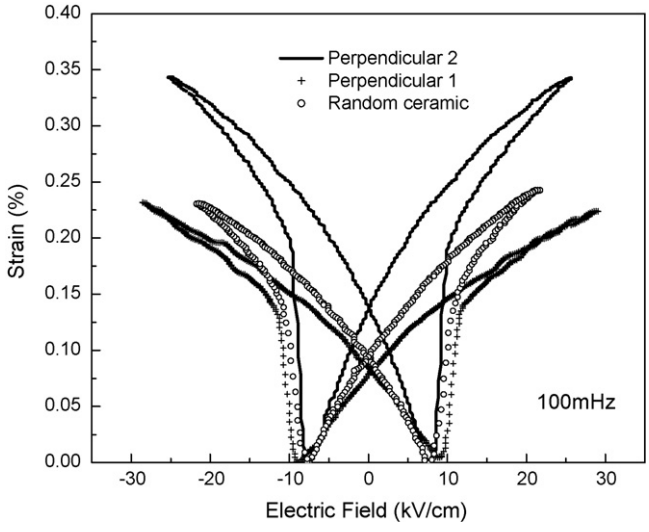

Fig. 8. Electric field-induced strain curves in axis parallel and perpendicular to the template for a sample of 0.6PMN–0.4PT prepared by RTGG plus hot pressing and 8 h of post-sinterization heat treatment and for a random 0.6PMN–0.4PT ceramic.

The piezoelectric coefficient d_{33} was determined from the slopes of the curves in Fig. 8 in the low field region (<10 kV/cm). The d_{33} of perpendicular 2 direction in the textured sample was 1100 pC/N, which is 31% higher than the d_{33} obtained for the randomic sample (840 pC/N) and 47% higher than the value obtained for perpendicular 1 direction (750 pC/N), which represents 1.47 of anisotropy factor. It means that [1 $\bar{1}$ 0] and [1 1 0] directions should present higher piezoelectric response than [0 0 1]. These results are comparable to the d_{33} = 1200 pC/N obtained for a 0.62PMN–0.38PT single crystal in [1 1 0] direction, which also presented higher piezoelectric coefficient along [1 1 0] than along [0 0 1] direction.[23]

The dielectric and piezoelectric properties of the textured PMN–PT ceramic together with results for a random ceramic and 0.62PMN–0.38PT single crystal are shown in Table 1.

4. Conclusions

Grain oriented PMN–PT were prepared by the combination of hot pressing and TGG or RTGG techniques, using perovskite $SrTiO_3$ single crystal fibers as templates. By the results we presented in this work it can be concluded that $SrTiO_3$ templates successful nucleate 0.6PMN–0.4PT anisotropic grains. Due to its easier preparation and efficiency, the RTGG texture technique was more attractive to work than TGG. After heat treatment, RTGG and hot pressing combined techniques produced highly dense monolithic textured PMN–PT ceramics, with values of dielectric constant ($\varepsilon_{max} = 5.0 \times 10^4$ and $\varepsilon_{RT} = 4.0 \times 10^3$), and piezoelectric coefficient (d_{33} = 1100 pC/N) comparable to single crystals. The textured 0.6PMN–0.4PT also presented higher levels of electric field-induced strain when compared to a random ceramic. The anisotropy between the three different monolithic sample axes was about 1.5.

Acknowledgements

The financial support of FAPESP and CNPq (Brazil) is gratefully acknowledged. The authors also thank Ms. Cleberson C. de Paula for the X-ray diffraction measurements, Mr. Eriton R. Botero for the electric field-induced strain measurements and Mr. Francisco J. Picon for the technical support.

References

1. Haertling, G., Ferroelectric ceramics: history and technology. *Journal of The American Ceramic Society*, 1999, **82**(4), 797–818.
2. Takenaka, T., Muramatsu, K. and Fujiu, T., Piezoelectric properties of $Pb(Zn_{1/3}Nb_{2/3})O_3$–$PbTiO_3$. *Ferroelectrics*, 1992, **134**, 133–138.
3. Sabolsky, E. M., James, A. R., Kwon, S., Trolier-McKinstry, S. and Messing, G., Piezoelectric properties of ⟨0 0 1⟩ textured $Pb(Mg_{1/3}Nb_{2/3})O_3$–$PbTiO_3$ ceramics. *Applied Physics Letters*, 2001, **78**(17), 2551–2553.
4. Holmes, M., Newnham, R. E. and Cross, L. E., Grain-oriented ferroelectric ceramics. *American Ceramic Society Bulletin*, 1979, **58**(9), 872.
5. Swartz, S., Schulze, W. A. and Biggers, J. V., Fabrication and electrical-properties of grain oriented $Bi_4Ti_3O_{12}$ ceramics. *Ferroelectrics*, 1981, **38**, 765–768.
6. Messing, G. L., Troiler-McKinstry, S., Sabolsky, E. M., Duran, C., Kwon, S., Brahmaroutu, B. *et al.*, Emplated grain growth of textured piezoelectric ceramics. *Solid State and Materials Sciences*, 2004, **29**(2), 45–96.
7. McHenry, D. A., Giniewickz, S. J., Jang, S. J., Bhalla, A. and Shrout, T. R., Optical properties of hot pressed relaxor ferroelectrics. *Ferroelectrics*, 1989, **93**, 351–359.
8. Swartz, S. L. and Shrout, T. R., Fabrication of perovskite lead magnesium niobate. *Materials Research Bulletin*, 1982, **17**(10), 1245–1250.
9. Uchino, K., *Ferroelectric Devices*. Marcell Dekker, Inc., New York, 2000.
10. Noheda, B., Piezoelectric materials overview. *Current Opinion in Solid State & Materials Science*, 2002, **6**(1), 27–34.
11. Zhou, Y. C., Liu, J. and Li, J. Y., Effective electromechanical moduli of ferroelectric ceramics with fiber texture. *Applied Physics Letters*, 2005, **86**, 262909-1–262909-3.
12. Kwon, S., Sabolsky, E. M., Messing, G. L. and Trolier-McKinstry, S., High strain, ⟨0 0 1⟩ textured $0.675Pb(Mg_{1/3}Nb_{2/3})O_3$–$0.325PbTiO_3$ ceramics: templated grain growth and piezoelectric properties. *Journal of the American Ceramic Society*, 2005, **88**(2), 312–317.
13. Sabolsky, E. M, Ph.D. thesis, The Pennsylvania State University, 2001.
14. Andreeta, E. R. M., Andreeta, M. R. B. and Hernandes, A. C., Laser heated pedestal growth of Al_2O_3/$GdAlO_3$ eutectic fibers. *Journal of Crystal Growth*, 2002, **234**, 782–785.
15. Andreeta, M. R. B., Hernandes, A. C., Cuffini, S. L., Guevara, J. A. and Mascarenhas, Y. P., Laser heated pedestal growth of orthorhombic $SrHfO_3$ single crystal fiber. *Journal of Crystal Growth*, 1999, **200**, 621–624.
16. Ardila, D. R., Andreeta, M. R. B., Cuffini, S. L., Hernandes, A. C., Andreeta, J. P. and Mascarenhas, Y. P., Single crystal $SrTiO_3$ fiber grown by laser heated pedestal growth method: influence of ceramic feed rod preparation in fiber quality. *Materials Research*, 1998, **1**(1), 11–17.
17. Stanciu, L. A., Kodash, V. Y. and Groza, J. R., Effects of eating rate on densification and grain growth during field-assisted sintering of α-Al_2O_3 and $MoSi_2$ powders. *Metallurgical and Materials Transactions A*, 2001, **32A**, 2633–2638.
18. Lente, M. H., Zanin, A. L., Andreeta, E. R. M., Garcia, D. and Eiras, J. A., Investigation of dielectric anomalies at cryogenic temperatures in the $(1-x)[Pb(Mg_{1/3}Nb_{2/3})O_3]$–$xPbTiO_3$ system. *Applied Physics Letters*, 2004, **85**(6), 982–984.
19. Zhao, X., Wang, J., Chew, K., Chan, H. L., Choy, C., Yin, Z. *et al.*, Composition dependence of piezoelectric constant and dielectric constant in the ⟨0 0 1⟩-oriented $[Pb(Mg_{1/3}Nb_{2/3})O_3]$–$PbTiO_3$ single crystals. *Materials Letters*, 2004, **58**, 2053–2056.
20. Wan, X., Zheng, R. K., Chan, H. L. W., Choy, C. L., Zhao, X. and Luo, H., Abnormal phase transitions for tetragonal $(1-x)[Pb(Mg_{1/3}Nb_{2/3})O_3]$–$xPbTiO_3$ single crystals at low temperature. *Journal of Applied Physics*, 2004, **96**(11), 6574–6577.
21. Zhang, Q. M., Wang, H., Kim, N. and Cross, L. E., Direct evaluation of domain-wall and intrinsic contributions to the dielectric and piezoelectric response and their temperature dependence on lead zirconate–titanate ceramics. *Journal of the Applied Physics*, 1994, **75**, 454–459.
22. Fousek, J., Litvin, D. B. and Cross, L. E., Domain geometry engineering and domain average engineering of ferroics. *Journal of Physics Condensed Matter*, 2001, **13**(1), L33–L38.
23. Xu, Z. J., Chu, R. Q., Li, G. R., Zeng, H. R., Yu, H. F. and Yin, Q. R., Strain anisotropy and piezoelectric response along ⟨0 0 1⟩ and ⟨1 1 0⟩ directions in PMN–38PT single crystal. *Materials Letters*, 2005, **59**, 1653–1655.